VOL. 13, NO. 4, FEBRUARY 2018 ISSN 1819-6608
ARPN Journal of Engineering and Applied Sciences

www.arpnjournals.com

COMPARATIVE STUDY FOR THE PREPARATION OF SUPERPARAMAGNETIC-CITRIC COATED MAGNETIC NANOPARTICLE AND FO-DESALINATION APPLICATION

Manal-Mounir[1], Eglal R[2], Hanaa Gadallah[1], A. A. Azab[3] and Hanaa M. Ali[1]
[1]Chemical Engineering Department, National Research Centre, Egypt
[2]Faculty of Science, Ain Shams University, Egypt
[3]Solid State Physics Department, National Research Centre, Egypt
E-Mail: hanaagadallah@hotmail.com

ABSTRACT

Forward osmosis as a unique low energy process, has achieved a greet attention, especially in desalination and water reuse applications. To make Forward osmosis more practical suitable draw solute with a good solubility, i.e. does not require energy, and non-toxicity properties have to be chosen or synthesised. In this study superhydrophilic, citric coated magnetic nanoparticles (Cc-MNP (1)) and Cc-MNP (2) were synthesised using a reverse co-precipitation and co-precipitation method, respectively. Both salts were demonstrated as an efficient draw solute in extracting water from saline water during-Forward osmosis experimental investigation. Forward osmosis performance-of both draw solutes was evaluated by using a commercial Forward osmosis membrane. The concentration effect of Cc-MNP (1) and Cc-MNP(2), feed salinity was investigated systematically. In Forward osmosis mode water flux of 28.6 L/m^{2}hr with 300 g/L Cc-MNP(1) and 21 L/m^{2}hr with 300 g/L Cc-MNP(2) were attained, also, it was found that water flux decreased with increasing feed salinity to become 5L/m^{2}hr with 300 g/L Cc-MNP(1) in case of using 35,000 ppm NaCl feed. The osmotic pressure of the optimum draw solute (Cc-MNP (1)) at a concentration of 300 g/L was 51.2 bar as evaluated from the freezing point depression measurements.

Keywords: forward osmosis, draw solutes, magnetite nanoparticles, reverse co-precipitation, citric coated, water desalination.

1. INTRODUCTION

Water lack which is one of the closely important issues owing to the increment of population growth in the high rate, climatechange and environmental deterioration, is threatening the life ofnationsall over the world [1-5]. The production of clean water from water reuse and brackish or sea-water-desalination will be required in the future as a result of population elevation. One of the most critical issues is the living standards that are being enhanced, and the expansion of industrial and agricultural fields put an effort on us to avoid all these foreseencrises [6, 7]. Theprocess of membrane filtration used widely inthefields of water purification. For wastewater treatment, low pressure-driven micro filtration (MF), ultrafiltration (UF) membranehas been broadly used [8], while for seawater desalination, high pressure drovenano-filtration (NF), reverse osmosis (RO) membranehas been applied [7]. Even though the broad applications of these membrane processes, labelled as an ‘‘energy intensive’’ technology, due to the application of high external hydraulic pressures, hence, the development of a sustainable and environmentally friendly waterproduction technology that consumes less energy is critically needed.

Forward osmosis (FO) has acquired an increasing concern similar to what the membrane technology has achieved in the previous 10 years. The theory of FO depends on using the natural osmotic phenomenon to draw water molecules through amembrane with a semipermeable character from a diluted feed solution to a higher concentrated solution that named the draw solution (DS). Hence, the dynamic force arises from the difference betweendraw solution and feed solution (FS) in their osmotic pressure [9].

Although the FO technologyhas shown a range of potential benefits, and lots of developments of its membrane structure have been made in order to-decrease-the effects of internal concentration polarization (ICP) [9-12], the lack of high performance FO membranes and suitable draw solutes with characteristics ofeasy restore and low cost are still hindering the developments [13]. Accordingly, when selecting a draw solution, the main criteria that have to be considered is namely the good solubility in water, solid state at ambient temperature and non-toxicity (in the field of potable water production), near neutral pH, compatibility with membrane surface and not expensive energy renewal [14].

Various chemicals (inorganic and organic) were suggested and tested to be draw solute. A number of inorganic chemicals such as $CaCl_2$,

NaCl and thermolytic ammonium salts were used and evaluated in termsof their performance and low restore costs as a draw water solutes by Achilli *et al.* [15]. $KHCO_3$,$MgSO_4$, and $NaHCO_3$were explored as draw solutes giving high FO performance, but their regeneration was difficult and costly, particularly when it comes to drinking water production. Besidess, these draw solutions, contain ions (Mg^{2+}, Ca^{2+},SO_4^{-2} and CO_3^{-2}) that are theprecursor to scaling on the membrane surface, when their concentrations increases abovethesolubility limit [16]. Ammonium bicarbonate has also been used as draw solute giving adequate water flux [17]. But inorderto make regeneration of this salt the ammoniumsalt should

thermally decompose at about 60 ^{o}C, beside thatthe reverse salt diffusion of ammonium bicarbonate is high comparedwith other draw agents, and thus it is not suitable for potablewater production as it may pose health hazards [15]. In addition, ifthe ambient temperature exceeds 30 ^{o}C. Clearly decomposition of ammonium salt may occur [16, 18]. Kessler and Moody [19] utilised a mix offructose and glucose solution as an organic FO draw solutes. Other organic components have also been utilised to be FO draw solutes, such as ethanol [20], polyethene glycol [21], and 2-methylimidazole-based compounds [22]. It should note that inorganic agents generally produce a higher waterflux compared with organic draw agents [16, 18]. In a new nanotechnological approach, hydrophilicmagnetic nanoparticles [1]are being tested as potential draw solutions [23]. Hydrophilic-magnetic nanoparticles can be rapidly separated from aqueous streams using a magnetic field. But, the main drawback is the agglomeration of the particles after recovery[2], which decreases the osmoticpressure and thus the flux [16].

The new developments of nano-materials[3,4] open a new doorfor the creation of ideal FO draw solutes. Fe_3O_4 MNPs canbeseparatedeasily from water by an external magnet field, thusthe stringent requirements for FO draw solutes can be met by creating high osmotic pressure and effective separation.-The polymer (2-pyrrolidone and PAA,-Mw = 1800) coated on Fe_3O_4 MNPs surface has been synthesised and used in FO process as a solute drawing water, but it is not enough for waterproduction from brackish water or seawater. This attributed to the large molecular weight of the polymer, which lowersits solubility in water. Therefore, it is reasonable that a low molecular weight organic functionalized Fe_3O_4 MNPs can generate higher osmotic pressure for water generation from brackish water. Citric acid as a natural acid-is-highly water soluble and can generate high osmotic pressureas inorganic salts. Some researchers have reported that citric acidcan be coated on Fe_3O_4 MNPs surface [24], the coating of nanoparticles have been demonstrated previously in application, which can be done with ease[5]

Herein, super-hydrophilic citric coated magnetic nanoparticles Cc-MNP(1) and Cc-MNP(2) were synthesised using a reverse co-precipitation and co-precipitation method, respectively. Also, FO performance utilising both the draw solutes was evaluated by using a commercial FO membrane. The effects of Cc-MNP (1) and Cc-MNP (2) concentration and feed salinity were investigated.

2. EXPERIMENTAL

2.1. Materials

i) All chemicals used are analytical grad and used without further purification. Iron (III) chloride hexahydrate ($FeCl_3.6H_2O$), iron (II) chloride tetrahydrate ($FeCl_2.4H_2O$, citric acid and sodium hydroxide (NaOH, 98%), were purchased from Sigma-Aldrich chemical Company (USA).

ii) For forward osmosis applications, FO woven thin film membrane from Hydration Technology Innovations Company (HTI) has been used, it is made of cellulose triacetate (CTA) embedded about a polyester mesh. This membrane has a thickness of about 50 μm, in addition it is smooth and hydrophilic [25]. The HTI membrane has been used in a number of studies, and it is known that these membranes are the best available membranes for FO applications [26, 27]; their characteristics are shown in Table-1.

Table-1. Characteristics of CTA FO membrane.

Item	Description
Thickness	50 μm
The water contact angles (active layer)	61.3°±0.8°
The water contact angles (support layer)	66.4°±1.3°
water permeability coefficient	1.07×10−12 m/s Pa
sodium chloride permeability coefficient	6.54×10−8 m/s

2.2. Experimental procedure

2.2.1. Preparation of citric coated Fe_3O_4 nanoparticle.

The citric coated Fe_3O_4 MNPs were synthesized by the co-precipitation of ferric and ferrous ions in alkaline solution. Briefly, The citric coated Fe_3O_4 (1) in first experiment were made as follows: 50 mL of well dissolved mixture of 7g citric acid, 17.3 g $FeCl_3{\cdot}6H_2O$ and 6.36 g $FeCl_2 \cdot 4H_2O$ solution were added drop by drop using a dropping funnel to 500 mL of 1 M NaOH solution in a three necked flask heated to 80 °C to hydrolyze the iron chlorides. The contents of the flask were stirred vigorously (315 rpm) for 60 min with a magnetic stirrer while being purged with nitrogen gas. Citric acid was coated on the surface of Fe_3O_4 MNPs via covalent binding interaction between the functional group of citric and the surface hydroxyl groups of Fe_3O_4 [28,23]. Leaving the flask to cool down, then the black product was separated by centrifugation, washed several times with DI water and finally washed with ethanol.

The final product was dried at 60 °C for 24 h. The citric coated magnetic nanoparticles by this method are labeled Cc-MNP(1).

In the second method, all the conditions were the same as the first one except that alkaline solution was added drop by drop using a dropping funnel to iron source solution mixed with citric acid in a three necked flask heated to 80 °C. The Citric coated Fe_3O_4 MNPs by this method are labeled Cc-MNP(2).

2.2.2. FO application

A bench scale system was prepared and set for our study with a membrane cell with two parallel channels. The schematic diagram of this set up is shown in Figure-1.

Draw and feed solutions have been re-circulated from their tanks at a cross-flow rate of0.857 l/min passing through the FO membrane cell and back to the tanks with the help of a piston dosing pump positive stroke, spring return.

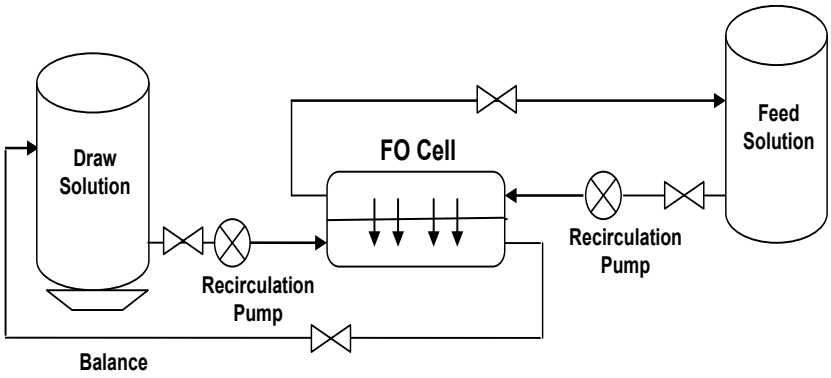

Figure-1. Schematic diagram of the bench-scale FO experimental setup.

The membrane cell consisted of CFO42 stainless steel 316 FO style cell and the real membrane area was 56 cm^2, the cell has symmetric channels on both sides of the membrane, dimensions of each channel were 2, 115, and 55 mm for height, length and width, respectively. Both of the draw and the feed solution were controlled independently. The DS tank has been placed on an analytical balance (Vibra, Pine Brook, NJ); the change of the DS weight with time was recorded and has been used for the calculation of the water flux through FO desalination process. TDS of the solutions has been measured with the conductivity meter of a model of Myronn L Ultrameter.

2.2.3 Measurement of water flux, salt rejection and reverse solute flux

A digital balance connected to a computer was used for monitoring the weight of pure water permeating across the membrane from the feed to the draw side. From the change of the mass of the draw solution with time the water flux (J_w) across the membrane will be determined by using equation (1):

$$J_w = \frac{\Delta W}{At} \quad (1)$$

Where J_w is water flux, $L/m^2h\Delta W$; weight change in time t, kg; ρ is density, kg/L; A is membrane are $am^2$and t is time interval, h; . A conductivity meter was used in the feed tank for determining the salt concentration. The salt flux can calculated by:

$$Js = \frac{C1m1 - Como}{At} \quad (2)$$

Where Js is the salt flux, $g/m^2h.C_1$, $m_1$is concentration of the feed and its mass after time t and C_o, m_o is the concentration of the feed and its mass at zero time.

2.3 Analysis

2.3.1. XRD

Analysis of X-ray diffraction (XRD) have been carried out by a Proker D8 advance X-ray diffractometer with Cu Kα radiation (λ = 1.5418A).” The XRD 2θ angles ranged from 10^o to 90^o”.

2.3.2. FTIR

Spectroscopic analysis by Infrared was carried out by Jasco 300E Fourier transform infrared spectrometer. “The spectrum has taken from 4000-400 cm^{-1},”

2.3.3. TGA

The weight loss of the synthetic draw solutes was analysed by thermo gravimetric analysis (TGA) with a SDT Q600 V20.9 Build20 made in USA

2.3.4. Zeta potential analysis

Zeta potential measurements are carried out using the Model DT-300 Zeta Potential probe (Dispersion Technology, Inc., New York, USA)

2.3.5 TEM

The microstructure of the nanoparticles have been analyzed by a JEOLe2100 at 200 KV high resolution transmission electron microscope (HRTEM).The sample powders for TEM have been dispersed in de-ionized water, the suspension was then dropped on carbon-copper grids.

2.3.6. VSM

The relation between magnetization and magnetic field was investigated at room temperature using a vibrating sample magnetometer (VSM; Lake Shore -7410-USA).From curve of (magnetization versus applied field, the applied field was between -20 and 20 KOe.), Ms (the saturation magnetization) was measured.

2.3.7 SEM

CTA membranes were examined using a Field Emission-SEM (QUANTA FEG 250) with a typical operating voltage of 20 kV

3. RESULTS AND DISCUSSIONS

3.1. Characterization of citric coated magnetic nanoparticles

3.1.1. Size and morphology

The preparation of magnetic Fe_3O_4 particles by co-precipitation and reverse co-precipitation methods are well known and widely used processes [1]. Figure-2a showthe X-ray diffraction (XRD) patterns for Cc-MNP(1) that indicate high crystalline structure. The diffraction peaks at 30, 35.4, 43, 53.4, 56.9, and 62.5° matches 220, 311, 400, 422, 511, and 440 planes of the cubic Fe_3O_4 lattice, respectively, These results agree with the XRD patterns of Fe_3O_4 nanoparticles reported in the literature [30] and the diffraction peaks at 28.6, 31.8, 33.35 and 37.5° show-thatcitric acid exists also [29], and confirmed formation of citric coated Fe_3O_4. This occurred also in case of Cc-MNP(2)in figure (2b) where diffraction peaks with slight shift in their position at 29.2,35.6, 53, 57 and 62.3° appeared, corresponded to 220, 311, 422,511 and440 planes of cubic Fe_3O_4lattice, respectively, in addition to diffraction peaks at 18.98, 28.04, 31.75 and 33.9°representing existence of citric acid-as a coat for Fe_3O_4[29].

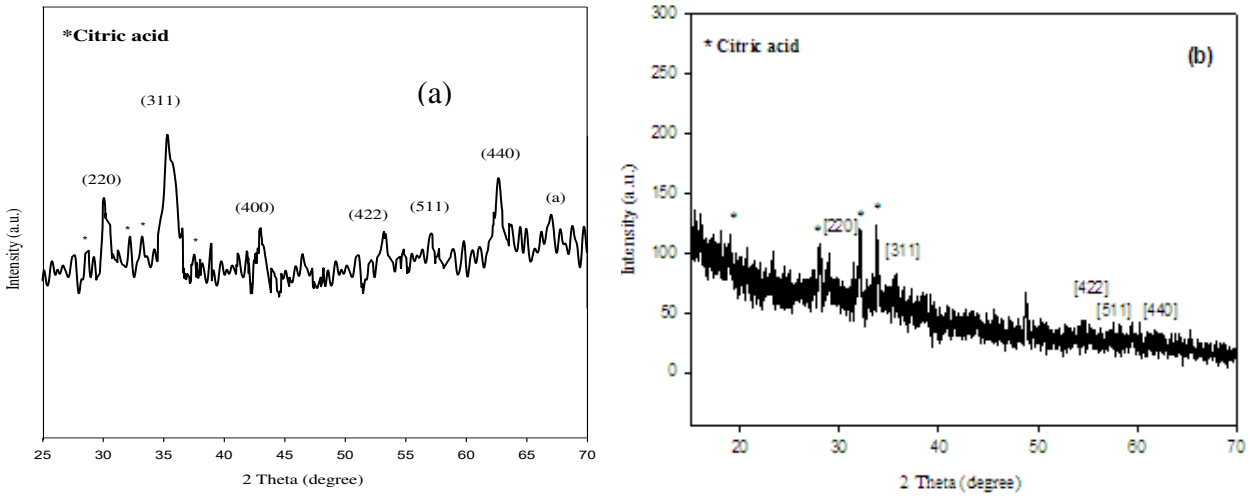

Figure-2. X-ray diffraction curves of (a) Cc-MNP(1) and (b) Cc-MNP(2).

3.1.2. FTIR

For further investigation of the surface of Cc-MNP(1)and Cc-MNP(2) nanoparticles, the spectra of IR for citric acid, Cc-MNP(1)and Cc-MNP(2) were measured. The results are shownin Figure-3, it can be clearly observed a great similarity in FTIR spectrum of Cc-MNP(1) and Cc-MNP(2) (curve a and b) to the IR spectrum of the citric acid an hydrous molecules (curvec). The peaks of stretching mode ν(as,COO^-) and ν(s,COO^-) ofcitric acid appeared at 1602 and 1388 cm^{-1}observed in part (a) of Figure-3, also it is observed in curve(b) at 1588, 1385.6 cm^{-1} and observed again at 1702 and 1396 cm^{-1}in part c of pure citric acid, respectively.-This indicates that the citratemolecules have been adsorbed on the surface of Fe_3O_4 NPs. Further-more, the ν(s, -CH)can also be observedin all curves a, b and c of Figure-3 at 2924, 2925.48 and 2936 cm^{-1}, respectively[23]. In addition, the bands at 598, 1033 and 3440 cm^{-1} in curve (a) and also observed at 610, 1072 and 3396.99 cm^{-1}in curve b are ascribed to Fe-O stretching mode [31-33], C-H vibrating mode and O-H vibrating-mode-[34], respectively. These results suggest that citrate is indeed an essential component of thecompound.

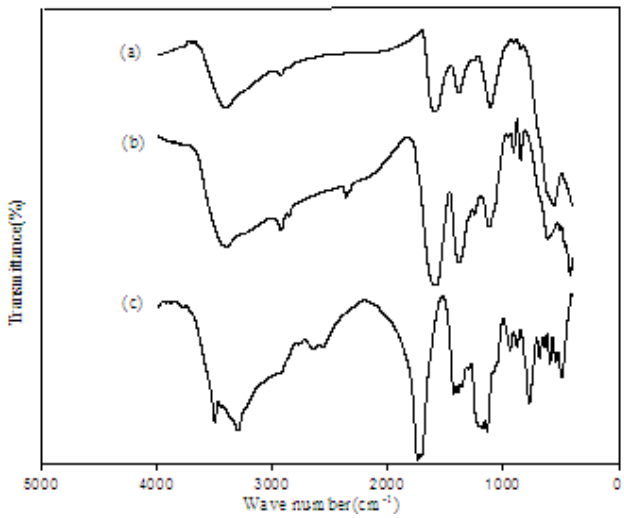

Figure-3. FTIR spectra of (a) Cc-MNP(1), (b) Cc-MNP(2) and (c) Citric acid

3.1.3. TGA analysis

Thermogravimetric analysis (TGA) wascarried out for measuring the organic content of the synthetic citrate coated MNPs, the results of TGA were appeared in

Figure-4 showing the weight losses of the Fe_3O_4 MNPs, Cc-MNP(1) and Cc-MNP(2), the weight loss curves observed in a range of temperatures of 160 to 800 °C of Cc-MNP(1) and Cc-MNP(2), are mainly attributed to the decomposition of the bonded citrate molecules to the magnetic nanoparticle surfaces [35]. The weight loss of bare MNP (1) was (3.6%) and bare MNP (2) was (5.4%) observed after a temperature higher than 100 °C were ascribed to water molecules loss. The determined organic content of Cc-MNP (1) and Cc-MNP (2) was 36.57 and 40.3%, respectively. This clears difference in the organic content coveredFe$_3$O$_4$insured the strong chemical bonds gathering the MNPs and citrate.

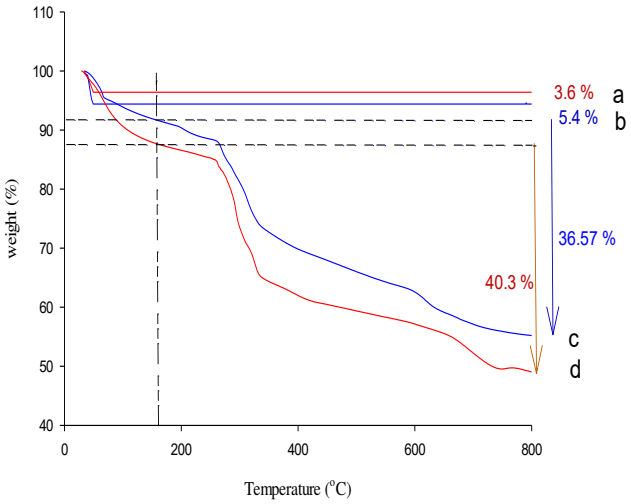

Figure-4. The thermogravimetric analysis (TGA) curves of: (a) bare MNP (1), (b) bare MNP (2), (c) Cc-MNP(1) and (d) Cc-MNP(2).

3.1.4. Zeta potential analysis

The effective method to prove the water stability of the nanoparticles is to characterise the surface charges of the bare-MNPs, Cc-MNP (1) and Cc-MNP (2) by zeta potentialanalysis as a function of pH from 3 to 11, Figure. (5) shows the same iso-electric point (IEP) for bare MNP at pH 6.8, as reported in the literature for magnetite [36,24], while Cc-MNP(1) and Cc-MNP(2) have negative zeta potentials of−40 and−46.6 mV at pH (7) as appeared in Figure-5. This observed phenomenon was likelycaused by adsorption of citrate molecules onto bare MNPs's surface, in which the surface-charges affected by the introduction of surface-functionalized carboxylategroups. By comparing the zeta potential curves for Cc-MNP (1) and Cc-MNP (2) one canunderstand that Cc-MNP (2) has much more carboxylate groupsthan does Cc-MNP (1). The zeta potential value changed to become more negativewith increasing pH due to the deprotonation of the carboxylate group of the citrate. This is because the pK_{a1} of citrate is 3.1, pK_{a2} is 4.8, and pK_{a3} is 6.4 [37], the more the negative charge the more enhancing ability for dispersing in water. The highly negative charge of both Cc-MNP(1) and Cc-MNP(2) at pH (7) increased their electrostatic repulsion and confirmedthe-stabilizationofthese draw solutes, and contributed to the potential application of them asdraw solutes for FO.

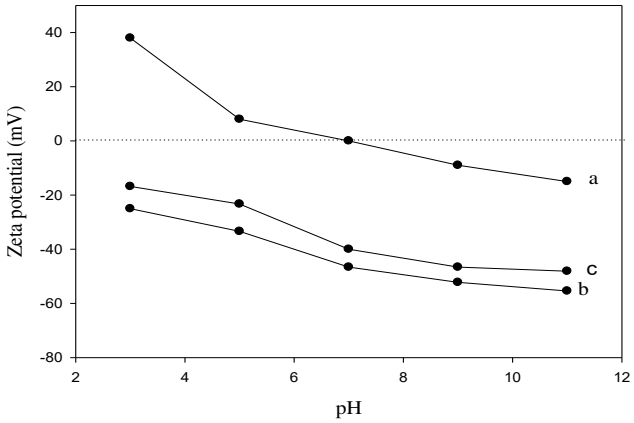

Figure-5. Change of Zeta potentials for: (a) bare MNP, (b) Cc-MNP(1) and (c) Cc-MNP(2) with pH values.
carboxylate groups (COOH)of citric acid showed specific adsorption onto bare MNP giving the shift in the IEP to low pH and providing high aqueous dispersion of both draw solutes at neutral pH. 3.1.5. TEM Images:

The Fe_3O_4 particles,-Cc-MNP(1) and Cc-MNP(2)in water solutionswith pH 7 have been testedwith TEM. In Figure-6, the images further confirming that Cc-MNP(1) and Cc-MNP(2) have a spherical morphology and good dispersive ability in water, This commonly occurs in case of co-precipitation of Fe-chloride salt solution in alkaline media, while Fe_3O_4particles' agglomeration immediately occursduring synthesis byprecipitation of Fe-chloride salt solution [38], the average particle sizes from the histograms of size distribution in Figure-7 were 32 and-2.7 nm for Cc-MNP(1) and Cc-MNP (2) respectively, nano-size magnetic particles withalargesurfacearea have high tendencyfor aggregation to reduce the surface energy. It is well known that the nanoparticle dispersions can be stabilized by the addition an effective coating, surfactantor polymer [4]. With the addition of citrate, the structure of the $Fe_3O_4$is considerably disturbed. The carboxylic groups of the citric molecule have a good coordination affinity for Fe ions, a reason for the high tendency of -COOH groups to be attachedto Fe_3O_4-nanocrystals surface, and hence, prevents them from the aggregation into large particles.

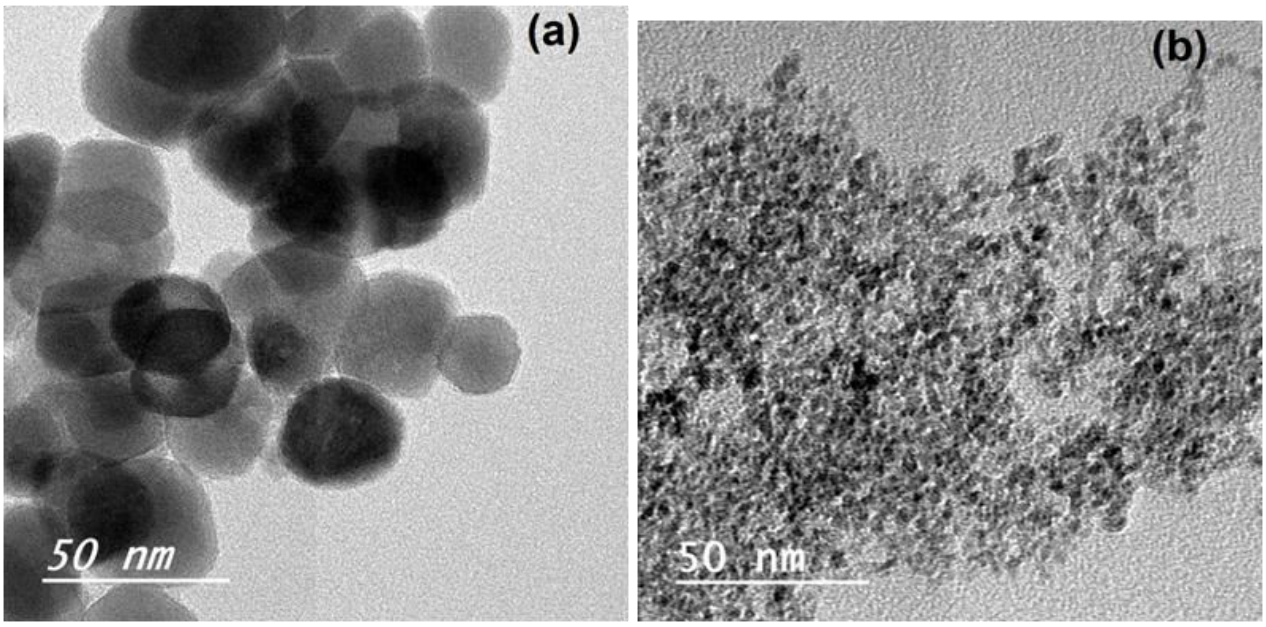

Figure-6. TEM images citric caped magnetic nanoparticles: (a) Cc- MNP(1) and (b)Cc-MNP(2).

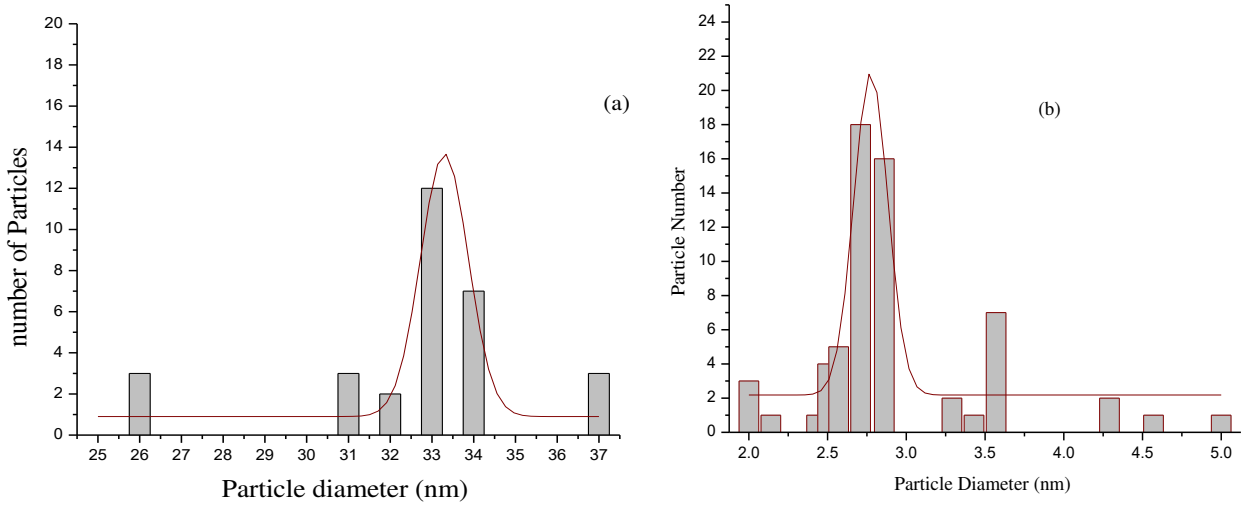

Figure-7. The particle size distribution of: (a) Cc-MNP (1) and (b) Cc-MNP(2).

3.1.6. Magnetic characteristics of the draw solute

From the hysteresis curves in Figure-8 for Cc-MNP(1) and Cc-MNP(2), the data showed that both of them exhibit super-paramagnetic behavior, with saturation magnetizations of 39.09 and 6.29 emu/g and,coercivity values of 29.67and 20.25 G respectively, also the retentivity values for Cc-MNP(1) and Cc-MNP(2) were 0.58 and 24.43emu/g respectively. Thegreat difference observed in the saturation magnetizations between the studied samples is attributed to two reasons, the first one is the great difference in size between them, where Cc-MNP(1) is larger than Cc-MNP(2) in particle size by ten times, it is known that the larger nanoparticle possess higher saturation magnetization for compounds, have the same composition [39-42]. The second reason is the difference in coating surface area between them [4], as Cc-MNP(2) is a very fine nanoparticle of 2.7 nm size, it has larger surface area and higher citric content consequently higher magnetic shielding, hence it is logic to have saturation magnetization value less than that of Cc-MNP(1). Inspect of citric coated on Fe_3O_4-surface, reduce its magnetic property, Cc-MNP(2) can be recovered from the water by the help of an external magnetic field.

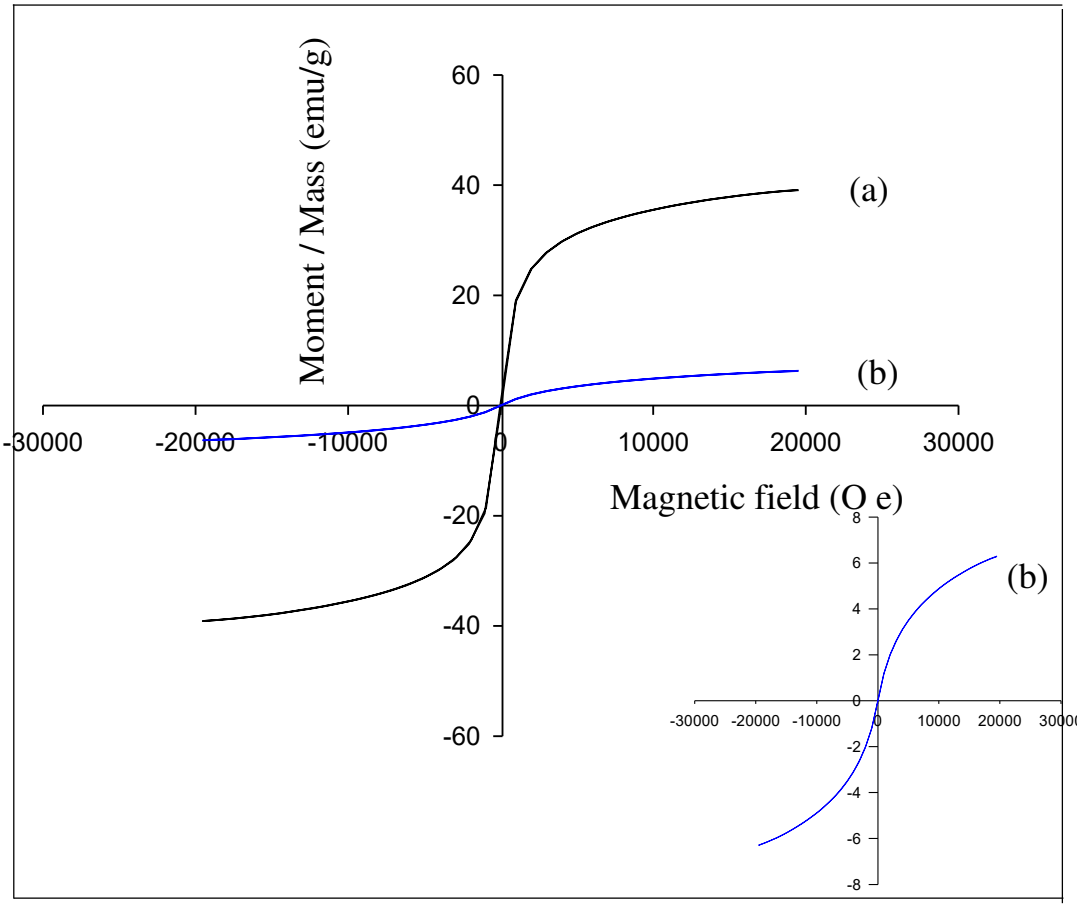

Figure-8. The magnetization curves of (a) Cc-MNP (1) prepared by reverse coprecipitation method and (b) Cc-MNP(2) prepared by normal coprecipitation method.

3.2. Determination of osmotic pressure, π

Ge, *et al*., measured the solutions (polyelectrolyte) osmotic pressure with Osmometer (model 3250 Advanced Instruments Inc) [43]. Freezing depression point has been measured by this instrument to determine their osmotic pressure ,the similar base was used in this study, for measuring the citric coated Fe_3O_4, MNPs solutions osmotic pressure. A known concentration of solutionwas frozen at (-35 ^oC), the profile of the temperature has been recorded to determine as T1. It is known that when one mole of ionic compound dissolved in 1kg of water the-osmotic pressure will increase by 17, 000 mm Hg and freezing point will depress by 1.86 ^oC [44]. And as the freezing point value of the pure solvent is known, ΔT= To - T1 can be obtained

$$\pi = \frac{\Delta T}{1.86} \text{x } 17{,}000 \text{mmHg} \quad (3)$$

$$\Delta T = 0.6 \text{ x n}(\frac{\text{g NaCl}}{100 \text{ g H2O}}),\ R^2 = 0.9991 \quad (4)$$

$$\Delta T = 0.14 \text{ x n}(\frac{\text{g Cc-MNP(1)}}{100 \text{ g H2O}}),\ R^2 = 0.998 \quad (5)$$

$$\Delta T = 0.17 \text{ x n}(\frac{\text{g Cc-MNP(2)}}{100 \text{ g H2O}}),\ R^2 = 0.995 \quad (6)$$

By the freezing point depression method, theosmotic pressure of Cc-MNP (1) and Cc-MNP(2) solutions were determined experimentally. NaCl solutions were also used to check the validity of this method, known amounts of NaCl or Cc-MNP(1) and Cc-MNP(2) powder were dissolved in 100 g water. From the temperature profile freezing point depression, ΔT was obtained, for example for 10g of Cc-MNP(1)/100g H_2O ΔT is 1.4^oC, as given in Figure-9, measured ΔT and calculated π values are given in Table-2. As clear fromequations (4), (5) and (6), linear relationships between concentration (g solute/100g (H_2O) and ΔT of NaCl, Cc-MNP(1) and Cc-MNP(2) were-detected. From-equations-(3) and (4) beside solution density of 1.03 g/cm the osmotic pressuresfor different concentration of NaCl were determined, these data agree with reported data determined by OLI Stream Analyzer™ [15].

Table-2. Freezing point depression of aqueous solution of NaCl and both synthetic magnetic draw solutes solutions.

n^a(NaCl)	Δ T (^{0}C)	π (bar)	n^a(solut)	Δ T (^{0}C)*	π (bar) *	Δ T (^{0}C)**	$\pi(bar)$ **
2.95	1.77	21.57	3.6	0.504	6.14	0.612	7.46
5.84	3.504	42.7	5.4	0.756	9.212	0.918	11.19
8.84	5.304	64.63	7	0.98	11.94	1.19	14.5
11.68	7.008	85.4	15	2.1	25.59	2.55	31.07
14.6	8.76	106.7	30	4.2	51.18	5.1	62.15

n^a–g solute in 100 g H_2O, * Cc-MNP(1) and ** Cc-MNP(2)

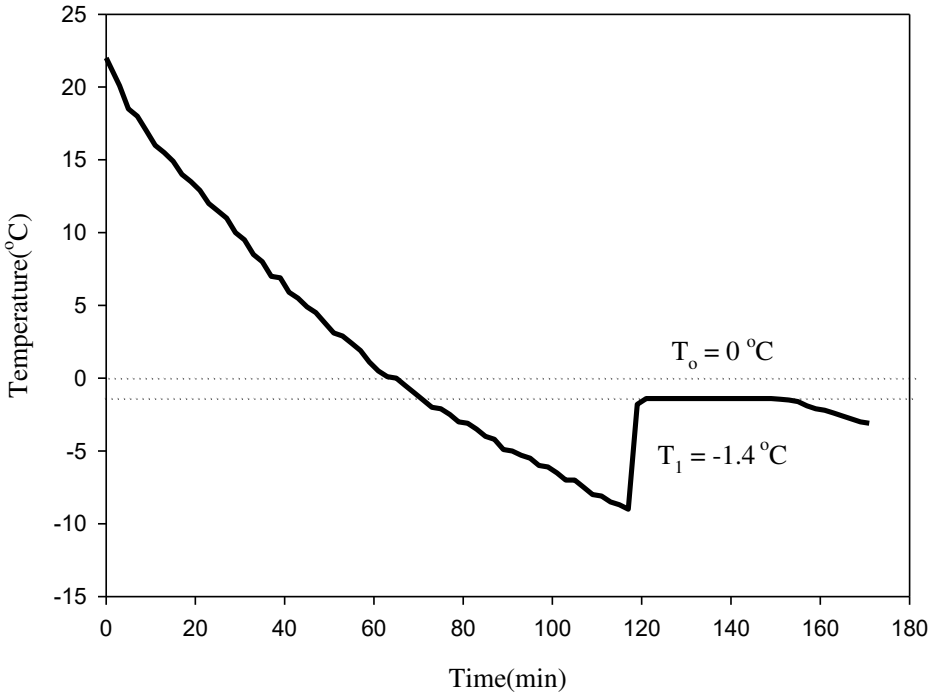

Figure-9. Freezing point temperature determination of Cc-MNP (2) solution (100 gm of Cc-MNP (2) in 1 kgH_2O).

3.3. FO performance

The FO process testing was conducted at one mode where the membrane active layer facing feed for avoiding aggravated fouling coming from pore-clogging in the support layer [15]. Figure-10 shows the effect of Cc-MNP (1) and Cc-MNP(2)concentrations as draw solutes on water flux and reverse salt flux through the FO membrane by using distilled water as feed solution, the concentrations were varied between 36 and 300 g/l. It was observed that the performance of Cc-MNP (1) higher than that obtained with Cc-MNP(2). In addition, high values of flux resulted at higher concentrations, then it decreased gradually by decreasing of concentration, in which at 300 g/l concentration the flux was reached to 28.6 and 21 L/m^2hr for Cc-MNP (1) and Cc-MNP (2) respectively, then it decreased to (21.4, 16.4), (16.9, 9.4), (11.9, 8.6) and (8.9,7.5) at concentrations of 150, 70, 54 and 36g/l. On the other hand, the reverse solute flux was increased gradually by increasing of concentration for both citric coated MNPs in which it increased from 0.088 to 2 g/m^2hr for Cc-MNP (1) and from 1.04 to 2.96 g/m^2hr for Cc-MNP (2).

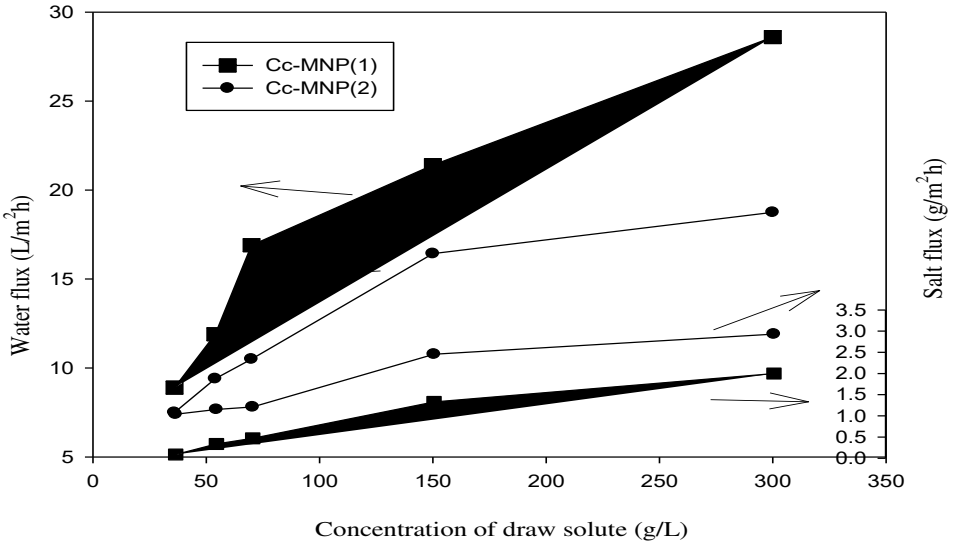

Figure-10. Concentration effect of Cc-MNP(1) and Cc-MNP(2) as draw solutes on water flux and salt flux (feed was DI water).

Figure-11 represents FO performance comparison of Cc-MNP (1) with Cc-MNP (2) in terms of water flux (curve a) and salt flux (curve b) at different osmotic pressure. It was found that, despite Cc-MNP(2) has higher osmotic pressure than Cc-MNP(1), where, at concentration of 30g/100g H_2O the osmotic pressure of Cc-MNP(1) and Cc-MNP(2) were 51.18 and 62.15 bar respectively, it is less in water flux values. This may attribute to the pores of the support skin (10-40 nm) which are much larger than the particle diameter of Cc-MNP (2) (2.7 nm). This makes the chance for blockage of membrane pores in the case of Cc-MNP (2) (Figure-12c)) more than Cc-MNP (1)as shown in Figure-12b, resulting in lowering of water flux.

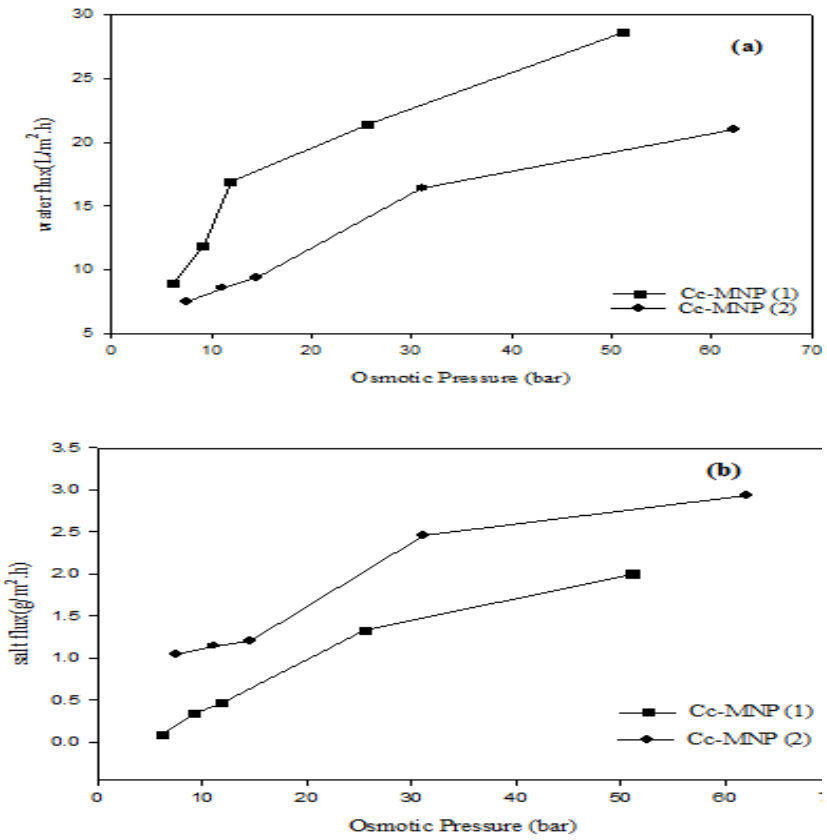

Figure-11. FO performance of Cc-MNP (1) and Cc-MNP(2) in terms of (a) water flux and (b) salt flux as a function of draw solutes osmotic pressure, (feed solution is DI water).

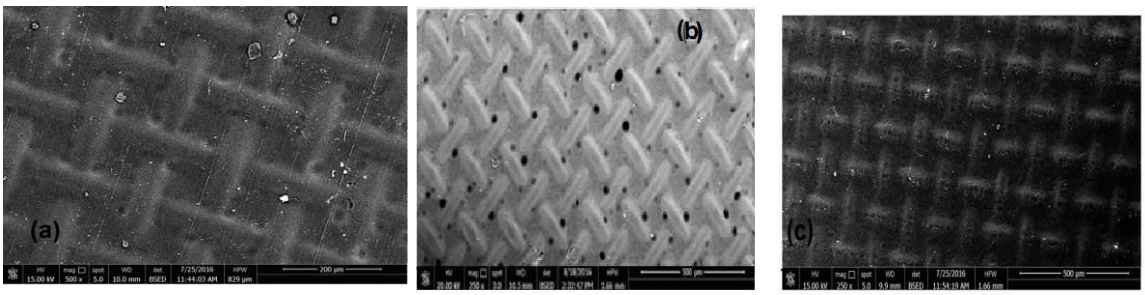

Figure-12. (a) SEM of original tested membrane, (b) SEM of tested membrane with Cc-MNP(1), (c) SEM of tested membrane with Cc-MNP(2).

Table-3 shows that the Cc-MNP (1) and Cc-MNP (2) draw solutes exhibit better performance than most of the other reported draw solutes of different types especially those have magnetic properties. With 0.3 g/mL Cc-MNP (1) and Cc-MNP(2) draw solutions, high values of water flux of 28.6 and 21 L/m^{2}hr were obtained, while, the negligible salt flux of 2 and 2.96 g/m^{2}hr, were observed.

Table-3. Notable draw solutes proposed for FO applications.

Draw solute used	Concentration	Operation mode	Water flux (LMH)	Reverse solute flux (GMH)	References
Cc-MNP(1)	300g/L	FO	28.6	2	This work
Cc-MNP(2)	300g/L	FO	21	2.96	This work
Cit-MNP	20mg/L	FO	17.3	-	24
NaCl	(1M)	TFC[a]	36	-	45
STPH	0.5 g/mL	(TFC) PRO	28.57	0.45	46
Polyacrylamide	0.04 g/mL	(TFC) PRO	4	0.04	47
Thermoresponsive copolymer	0.5 g/mL	(TFC) PRO	4	-	48
PAMAM-COONa	0.5 g/mL	(TFC) PRO	29.7	8.86	49
Responsive ionic liquid (P4444DMBS) [b]	0.5 g/mL	(TFC[c]) PRO	4	-	50
Ferric complex (Fe-OA),	0.39 g/mL	TFC-PES PRO)	27.5	0.28	51
Ferric complex (Fe-CA),	2M	TFC-PES[d] PRO	40.5	0.13	52
Cobaltous complex (Co^{2-} CA)	2M	TFC-PES PRO	24.6	0.13	52

[a] Thin film composite membrane (TFC); [b]Tetrabutylphosphonium 2,4-dimethylbenzenesulfonate (P4444DMBS); [c] Feed solution: 0.6 NaCl; [d] Thin film composite membrane with polyether sulfone as substrate (TFC-PES).

3.4. Application with different NaCl concentrations

Generally, the optimum draw solute was chosen on basis of high water flux, low reverse salt flux and low fouling effect on the membrane. As illustrated in the previous section, Cc-MNP (1) was found to be the best one, so it was chosen for the application.

FO performance of Cc-MNP (1) as for draw solute at a concentration of 300 g/L with different concentration of saline feed-were investigated. As appeared in-Figure(13),it is clear that water flux decreased gradually by increasing of feed concentration, in which it decreased from 28.6 L/m^{2}hr with distilled water to 19.95, 12.8, 8.9 and 5L/m^{2}hr at NaCl concentrations of 3000 ppm, 7000 ppm, 12000 and 35000 ppm.

The results are in good finding with literature [53, 54]; they demonstrated the feed solution concentrations effect on FO performance, they deduced that the decrease in water flux when feed concentration increases-was-due to the decrease in the net-osmotic pressure"-osmotic pressure difference between the feed and the draw solution", the increase in feed concentrations increases the feed osmotic pressure, hence reduces the overall driving force for water transport.

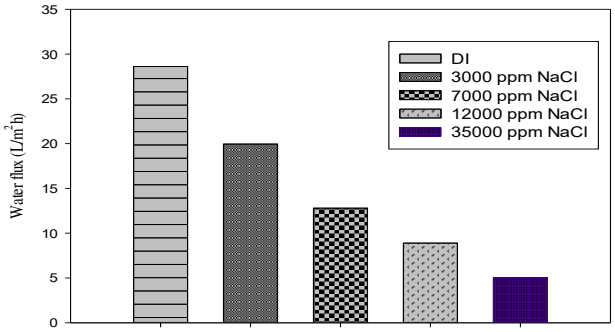

Figure-13. FO performance (water flux) of 300 g/ L Cc-MNP(1) as draw solution and the feed solutions were both DI water and different concentration of NaCl .

4. CONCLUSIONS

In this work super-paramagnetic citric coated Fe_3O_4-MNPs with high water solubility and ability for generating high osmotic pressure, were,synthesised,by two methods and.applied as draw solutes in FO process. The citric coated Fe_3O_4 MNPs were characterised by XRD, FTIR, TGA, TEM, VSM and zeta potential. The formation of surface coated MNP with citric acid was confirmed by XRD, FTIR and TGA. The produced particles were proven to be in nano-size, good dispersive in water, and having good saturation magnetisations of 39.09 emu/g.FO performance of both Cc-MNP(1)and Cc-MNP(2) showed that these, draw solutions exhibit better performance than most of the other reported draw solutes of different types especially those having magnetic properties.

With 0.3 g/mL Cc-MNP(1) and Cc-MNP(2) draw solutions, a high water fluxes of 28.6 and 21 LMH were obtained, while, the negligible salt fluxes of 2 and 2.96 gMH were observed.

REFERENCES

[1] The Global Risks Report 2016, 11th Edition.

[2] Bates B., Kundzewics Z.W., WuS. 2008. Climate Change and Water, Technical Paper of the Intergovernmental Panel on Climate Change, IPCC Secretariat, Geneva, J. Palutik. p. 201.

[3] 2016. High and Dry Climate Change, Water, and the Economy.

[4] McGinnis R.L., Elimelech M. 2008. Global challenges in energy and water supply: the promise of engineered osmosis, Environmental Science and Technology. 42: 8625-8629.

[5] Shannon M.A., Bohn P.W., Elimelech M., Georgiadis J.G., Marinas B.J., Mayes A.M. 2008. Science and technology for water purification in the coming decades, Nature. 452: 301-310.

[6] Glueckstern P., Priel M., Gelman E., Perlov N. 2008. Waste water desalination in Israel, Desalination. 222: 151-164.

[7] Greenlee L.F., Lawler D.F., Freeman B.D., Marrot B., Moulin P. 2009. Reverse osmosis desalination: water sources, technology, and today's challenges, Water Research. 43: 2317-2348.

[8] Jacangelo J.G., Trussell R.R., Watson M. 1997. Role of membrane technology in drinking water treatment in the United States, Desalination. 113: 119-127.

[9] Yip N.Y., Tiraferri A., Phillip W.A., Schiffman J.D., Elimelech M. 2010. High performance thin-film composite forward osmosis membrane. Environmental Science and Technology. 44: 3812-3818.

[10] Wang K.Y., Ong R.C., Chung T.S, 2010. Double-skinned forward osmosis membranes for reducing internal concentration polarization within the porous sublayer. Industrial and Engineering Chemistry Research. 49: 4824-4831.

[11] Su J., Chung T.S. 2011. Sublayer structure and reflection coefficient and their effects on concentration polarization and membrane performance in FO processes. Journal of Membrane Science. 376: 214-224.

[12] Zhang S., Wang K.Y., Chung T.S., Jean Y.C., Chen H.M. 2011. Fundamental understanding of formation mechanism of cellulose ester membranes for the application in forward osmosis. Chemical Engineering Science. 66: 2008-2018.

[13] Chung T.S., Zhang S., Wang K.Y., Su, J., Ling M.M. 2012. Forward osmosis processes: Yesterday, today and tomorrow, Desalination. 287: 78-81.

[14] Forward osmosis processes: yesterday, today and tomorrow. Desalination. doi:10.1016/j.desal.2010.12.019.

[15] Achilli A., Cath T.Y., Childress A.E. 2010. Selection of inorganic-based draw solutions for forward osmosis applications, J. Membr. Sci. 364: 233-241.

[16] Chekli L., Phuntsho S., Shon H.K., Vigneswaran S. 2012. Kandasamy J., Chanan A., Areview of draw solutes in forward osmosis process and their use in modern applications, Desalin. Water Treat. 43: 167-184.

[17] McCutcheon J.R., McGinnis R.L., Elimelech M. 2005. A novel ammonia-carbondioxide forward (direct) osmosis desalination process, Desalination. 174: 1-11.

[18] Ng H.Y., Tang W. 2006. Forward (direct) osmosis: a novel and prospective process forbrine control, Proc. Water Environ. Fed. 4345-4352.

[19] Kessler J.O., Moody C.D. 1976. Drinking water from sea water by forward osmosis, Desalination. 18: 297-306.

[20] McCormickP., Pellegrino J., Mantovani F., Sarti G., 2008, Water, salt, and ethanoldiffusion through membranes for water recovery by forward (direct) osmosisprocesses, J. Membr. Sci. 325: 467-478.

[21] Petrotos K.B., Quantick P., Petropakis H. 1998. A study of the direct osmotic concentration of tomato juice in tubular membrane-module configuration. I. The effect of certain basic process parameters on the process performance, J. Membr. Sci. 150: 99-110.

[22] Yen S.K., MehnasHaja F. N, Su M., Wang K.Y., Chung T.-S, 2010, Study of draw solutes using 2-methylimidazole-based compounds in forward osmosis, J.Membr. Sci. 364: 242-252.

[23] Bai H., Liu Z., Sun D.D. 2011. Highly water soluble and recovered dextran coatedFe3O4 magnetic nanoparticles for brackish water desalination, Sep. Purif.Technol. 81: 392-399.

[24] Yonghun N., Seungheon Y., Seockheon L. 2014. Evaluation of citrate-coated magnetic nanoparticles as draw solute for forward osmosis. Desalination. 347: 34-42.

[25] McCutcheon J.R., McGinnis R.L., Elimelech M. 2006. Desalination by ammonia–carbon dioxide forward osmosis: Influence of draw and feed solution concentrations on process performance, J Membr Sci. 278: 114-123.

[26] Jarusutthirak C., Amy G., Croué J.P. 2002. Fouling characteristics of wastewater effluent organic matter (EfOM) isolates on NF and UF membranes Desalination. 145: 247-255.

[27] Wang Y., Wicaksana F., Tang C.Y., Fane A.G. 2010. Direct microscopic observation of forward osmosis membrane fouling. Environ SciTechnol. 44: 7102-7109.

[28] Banerjee S.S., Chen D.H. 2007. Fast removal of copper ions by gum arabic modified Magneticnano-adsorbent, Journal of Hazardous Materials. 147: 792-799.

[29] Lafontaine A., Sanselme M., Cartigny P.,Cardinael Y., Coquerel G. 2013. Characterization of the transition between the monohydrate and the anhydrous citric acid, J. Therm Anal Calorim. 112: 307-315.

[30] Hui C., Shen C., Yang T., Bao L.,Tian J., Ding H., LiC., Gao H.J. 2008. Large-scale Fe_3O_4 nanoparticles soluble in water synthesized by a facile method, J. Phys. Chem. C. 112: 11336–11339.

[31] Waldron R.D. 1955. Infrared spectra of ferrites, Physical Review. 99: 1727-1735.

[32] Shinde U.B., Sagar, Shirsath E., Patange S.M., Jadhav S.P., Jadhav K.M., Patil V.L. 2013. Preparation and characterization of Co2þ substituted Li-Dyferriteceramics, Ceramics International. 39: 5227-5234.

[33] Le-Zhong Lin, Xiao- QiangTu, Rui Wang, Long Peng. 2015. Structural and magnetic properties of Cr-substituted NiZnCo ferrite nanopowders. Journal of Magnetism and Magnetic Materials 381:328–331.

[34] Balavijayalakshmi J.,Suriyanarayanan N.,Jayaprakash R., Gopalakrishnan V. 2013. Effect of concentration on dielectric properties of Co-Cu ferrite nano particles, Physics Procedia. 49: 49-57.

[35] Cheng C., Wen Y., Xu XGu., H. 2009. Tunable synthesis of carboxyl-functionalized magnetite nanocrystal clusters with uniform size, J. Mater. Chem. 19: 8782-8788.

[36] Tombácz E., Libor Z., Illés E., Majzik A., KlumppE. 2004. The role of reactive surface sites and complexation by humic acids in the interaction of clay mineral and iron oxideparticles, Org. Geochem. 35: 257-267.

[37] Campelj S., Makovec D., Drofenik M. 2008. Preparation and properties of water-based magnetic fluids, J. Phys. Condens. Matter. 20: 204101-204105.

[38] Massart R. 1981. Preparation of aqueous magnetic liquids in alkaline and acidic media, IEEE Trans. Magn. 17: 1247-1248.

[39] Nagar H., Kulkarni N.V., Karmakar S., Sahoo B., Banerjee I., Chaudhari P.S., Pasrichab R., Dasc A.K., Bhoraskar S.V., Datea S.K., Keuned W. 2008. MOssbauer spectroscopic investigations of nanophase iron oxides synthesized by thermal plasma route, Mater. Charact. 59:1215.

[40] Anil Kumar P.S., Shrotri J.J., Kulkarni S.D., Deshpande C.E., Date S.K. 1996. Low temperature synthesis of Ni0.8Zn0.2Fe2O4 powder and its characterization Mater. Lett. 27: 293-296.

[41] Caizer C., Stefanescu M. 2003. Nanocrystallite size effect on sigma(s) and H-c in nanoparticle assemblies Physica B. 327: 129-134.

[42] Hong R.Y., Feng B., Chen L.L., Liu G.H., Li H.Z., Zheng Y., Wei D.G. 2008. Synthesis, characterization and MRI application of dextran-coated Fe_3O_4 magnetic nanoparticles, Biochemical Engineering Journal. 42: 290-300.

[43] Ge Q.C., Su J. C., Amy G. L., Chung T. S. 2012. Exploration of polyelectrolytes as draw solutes in forward osmosis processes, Water Res. 46: 1318-1326.

[44] Jintang Duan, Eric Litwiller, Seung-Hak Choi, Ingo Pinnau, 2014, Evaluation of sodium lignin sulfonate as draw solute in forward osmosis for desert restoration, Journal of Membrane Science. 453: 463-470.

[45] The membrane technical data sheet. Available online: http://www.htiwater.com/shop/research/form.php (accessed on 12 December 2012).

[46] Long Q. W. and Wang Y. 2015. Sodium Tetraethylenepentamine Heptaacetate as Novel Draw Solute for Forward Osmosis-Synthesis, Application and Recovery, Energies. 8: 12917-12928.

[47] Zhao P.; Gao B.; Xu S.; Kong J.; Ma D.; Shon H.K.; Yue Q.; Liu P. 2015. Polyelectrolyte-promoted forward osmosis process for dye wastewater treatment-Exploring the feasibility of using polyacrylamide as draw solute. Chem. Eng. J. 264: 32-38. [CrossRef].

[48] Zhao D.; Wang P.; Zhao Q.; Chen, N.; Lu, X. 2014. Thermoresponsive copolymer-based draw solution for seawater desalination in a combined process of forward osmosis and membrane distillation. Desalination. 348: 26-32. [CrossRef].

[49] Zhao D.; Chen S.; Wang P.; Zhao Q.; Lu X.A. 2014. Dendrimer-Based Forward Osmosis Draw Solute for Seawater Desalination. Ind. Eng. Chem. Res. 53:16170-16175. [CrossRef].

[50] Cai Y.; Shen W.; Wei J.; Chong T.H.; Wang R.; Krantz W.B.; Fane A.G.; Hu X. 2015. Energy-efficient desalination by forward osmosis using responsive ionic liquid draw solutes. Environ. Sci. Water Res. Technol. 1: 341-347. [CrossRef].

[51] Ge Q.; Chung T.-S. 2015. Oxalic acid complexes: Promising draw solutes for forward osmosis (FO) in protein enrichment. Chem. Commun. 51: 4854-4857. [CrossRef] [PubMed].

[52] Ge Q.; Fu F.; Chung T.-S. 2014. Ferric and cobaltous hydroacid complexes for forward osmosis (FO) processes. Water Res., 58: 230–238. [CrossRef] [PubMed].

[53] Cui Y, Ge Q, Liu X, Chung T. J 2014. Novel forward osmosis process to effectively remove heavy metal ions, Membr. Sci. 467: 188-194.

[54] Ali S. S., Sabry R., Gadallah H. and Ali H. M. 2016. Investigation of Ammonium Sulfate/Ammonium Di-Hydrogen Phosphate fertilizers as Draw Solute for Forward Osmosis Desalination, Research Journal of Pharmaceutical, Biological and Chemical Sciences, January-February. 7: p. 760.